cognizancejournal.com
Mohammad Daud Ahmadzai *et al*, Cognizance Journal of Multidisciplinary Studies, Vol.5, Issue.1, January 2025, pg. 644-653
(An Open Accessible, Multidisciplinary, Fully Refereed and Peer Reviewed Journal)
ISSN: 0976-7797
Impact Factor: 5.183
Index Copernicus Value (ICV) = 77.57

Formation of OAM Beams by Circular Polarization Ceramic Antenna Array

Mohammad Daud Ahmadzai

Dean of Faculty of Electro Mechanic Kabul Polytechnic University (KPU), Kabul, Afghanistan
*Corresponding author: am.daudahmadzai@gmail.com

Noorullah Faizulbari

Lecturer & Assistant, Faculty of Electro Mechanic Kabul Polytechnic University (KPU), Kabul, Afghanistan

Mohammad Ismail Ahmadzai

4th year student, Faculty of Compueter Science Kabul Polytechnic University (KPU), Kabul, Afghanistan

DOI: 10.47760/cognizance.2025.v05i01.049

Abstract: Orbital angular momentum (OAM) beams can be generated at various microwave frequencies through using antenna array. However, the intricacy of system and incapacity to transmit over long distances limit the applications of OAM beams in radio domain. Here, a significantly simplified global positioning system (GPS) ceramic antenna array is employed to generate OAM beams without the help of phase shifting devices. Simulation of the GPS ceramic antenna array proves that the OAM beams with the mode of ±1 show small divergence angle and very standard spiral phase delivery. To test the transmission competence of the proposed antenna array, a measurement system which can detect the One-dimension spatial delivery of electromagnetic characteristic for the OAM beams is set up. Even considering the vast loss in cables and power divider, the receiving antenna still can receive the electromagnetic characteristic of the OAM beams at a place more than 2 m away from the antenna array. Experimental results presented in this paper demonstrate the excellent presentation of the OAM beams when generated with the proposed ceramic antenna array formation.

Keywords: OAM Beams, Orbital angular momentum, Circular Polarization, Ceramic Antenna Array

Introduction

Total angular momentum includes spin angular momentum and orbital angular momentum (OAM) [1]. Because of their unique spatial intensity and phase profile, optical OAM beams have been receiving a lot of interest [2–4]. OAM beams display their unique advantages, particularly in rotating small particles [8], optical imaging [6,7], trapping particles [5], and other fields [9–11]. The OAM beams with different promulgating modes are mutually orthogonal with each other [12], which offers the possibility to increase the capacity of radio communication under certain situations [13]. Recently, the generation of OAM beams in microwave range has been reported in many works [14–16]. OAM beams acquired a lot of attention in the microwave

cognizancejournal.com
Mohammad Daud Ahmadzai *et al*, Cognizance Journal of Multidisciplinary Studies, Vol.5, Issue.1, January 2025, pg. 644-653
(An Open Accessible, Multidisciplinary, Fully Refereed and Peer Reviewed Journal)
ISSN: 0976-7797
Impact Factor: 5.183
Index Copernicus Value (ICV) = 77.57

industry as a possible way for improving spectrum efficiency [17–19]. Since the first simulation proposed by Thidé [20], various methods have been developed to generate OAM radio beams [21], such as spiral phase plates [22,23], spiral reflectors [24], meta surface [25] and antenna arrays [26–28]. While the first three approaches can successfully transform a plane wave into an OAM radio wave reflection, the intrinsic complex processing and single operational frequency restrict their further development. The antenna array conformed circular delivery, generally needs a feed network to provide appropriate signals for each element. To generate an OAM beam, these signals are required to get the same amplitude and suitable phase shift. The specific phase shift between adjacent antennas depends on the mode of the OAM beam and the number of antennas in the antenna array. As a consequence, the antenna systems in generating OAM beams are too complex to meet these conditions. To simplify the OAM antenna array, a system shaped by global positioning system (GPS) ceramic antennas that evades the use of phase shifting devices is proposed. The separate advantages of GPS ceramic antenna such as circular polarization, high precision, low profile, etc. can make this antenna system perform better. In particular, the mixture of circular polarization and circular distribution is the key point to comprehend the automatic phase modification. The utilization of power divider and coaxial line connecting make the proposed system simple and flexible. Furthermore, the problem of deviation angle of OAM beam can also be highly improved by such a simplified antenna array system. Section 2 describes the design of GPS ceramic antenna and its polarized characterization. Section 3 presents the simulations and measurements of generating OAM beams by the GPS ceramic antenna array. Finally, in Section 4, we draw the conclusions.

Design and Characterization of GPS Ceramic Antennas

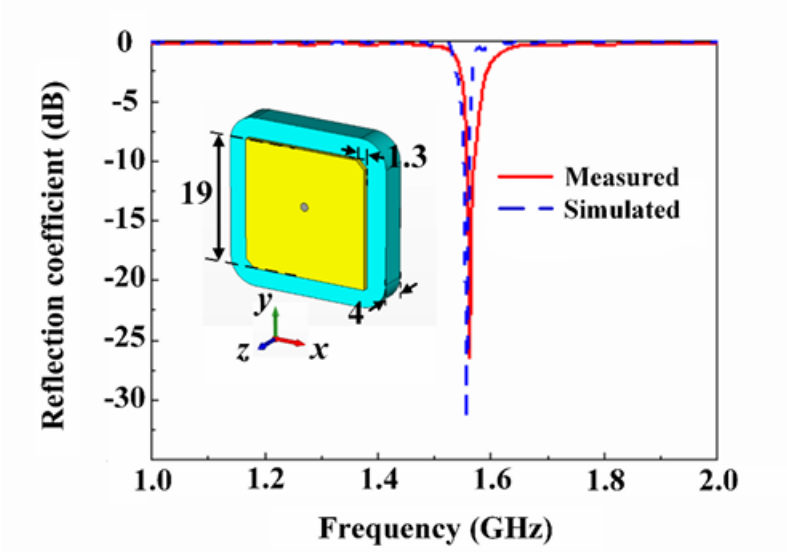

Fig. 1.Reflection Coefficients of the GPS Ceramic Antenna: Measured and Simulated Results

cognizancejournal.com
Mohammad Daud Ahmadzai *et al*, Cognizance Journal of Multidisciplinary Studies, Vol.5, Issue.1, January 2025, pg. 644-653
(An Open Accessible, Multidisciplinary, Fully Refereed and Peer Reviewed Journal)
ISSN: 0976-7797
Impact Factor: 5.183
Index Copernicus Value (ICV) = 77.57

To date, cut corner rectangle is a simple structure that is extensively used in the design of circular polarization (CP) antenna [29,30]. Its side length determines the resonant frequency of CP antenna. Cutting corner and center counterbalance of feed point aim to achieve the CP of antenna. Here, the resonant frequency of the antenna is determined to be 1.550 GHz to meet the application of GPS. By means of calculation and optimization, the side length of radiation patch and cut corner are set to be 19 mm and 1.3 mm, respectively. The proposed antenna is designed on a ceramic substrate with a thickness of 4 mm and the relative permittivity of 21.4. And the radius of the chamfer is set to 4 mm to protect the antenna. Only in y direction, the center offset gets a non-zero value of 1.1 mm. The radiation patch, chamfered rectangular ceramic dielectric layer and ground plane together compose the GPS ceramic antenna. Numerical predictions of the reflection coefficients for the GPS ceramic antenna were made using the commercial time-domain package CST Microwave Studio TM. Figure 1 shows the measured and simulated results. The inserted illustration is the configuration of the GPS ceramic antenna. In the simulation, all boundaries are set as open (add space), and the direction of propagation is along z-axis. In the untried setup, the proposed antenna is operated at 1.550 GHz frequency, which is applicable for GPS. From Figure 1, it can be seen that the measured result coincides well with the simulated one, which demonstrates the reasonableness of the proposed design. Figure 2(a) display the axial ratio of the proposed antenna from 1.540 to 1.560 GHz. At its resonant frequency of 1.550 GHz, the axial ratio is less than 3 DB. Consequently, this antenna can be regarded as a CP antenna. In Figure 2(b), the nearly circular radiation pattern of the GPS ceramic antenna in x-y plane at the resonant frequency of 1.550 GHz well illustrates the omnidirectional properties of the proposed antenna.

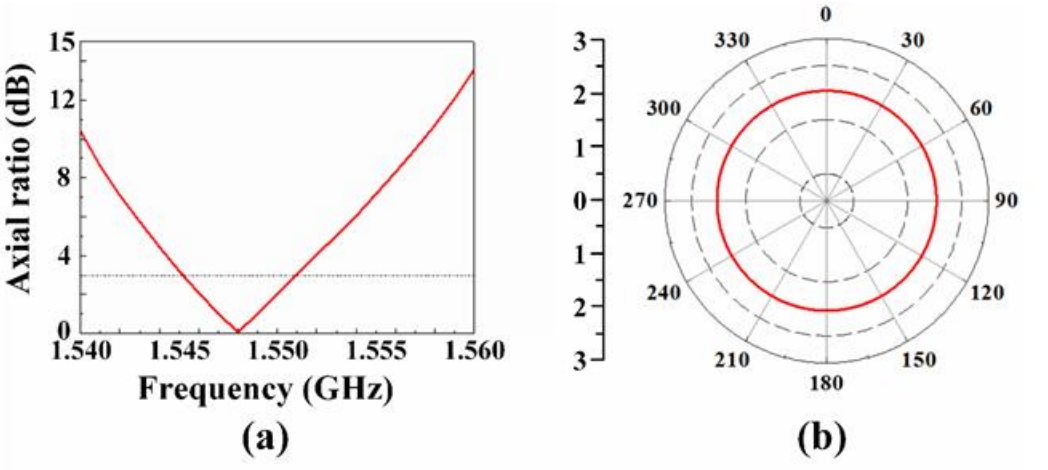

Fig. 2. (a) Simulated Axial Ratio of the GPS Ceramic Antenna.
(b) Simulated Radiation Pattern of the GPS Ceramic Antenna at 1.550 GHz in the x-y Plane.

cognizancejournal.com
Mohammad Daud Ahmadzai *et al*, Cognizance Journal of Multidisciplinary Studies, Vol.5, Issue.1, January 2025, pg. 644-653
(An Open Accessible, Multidisciplinary, Fully Refereed and Peer Reviewed Journal)
ISSN: 0976-7797
Impact Factor: 5.183
Index Copernicus Value (ICV) = 77.57

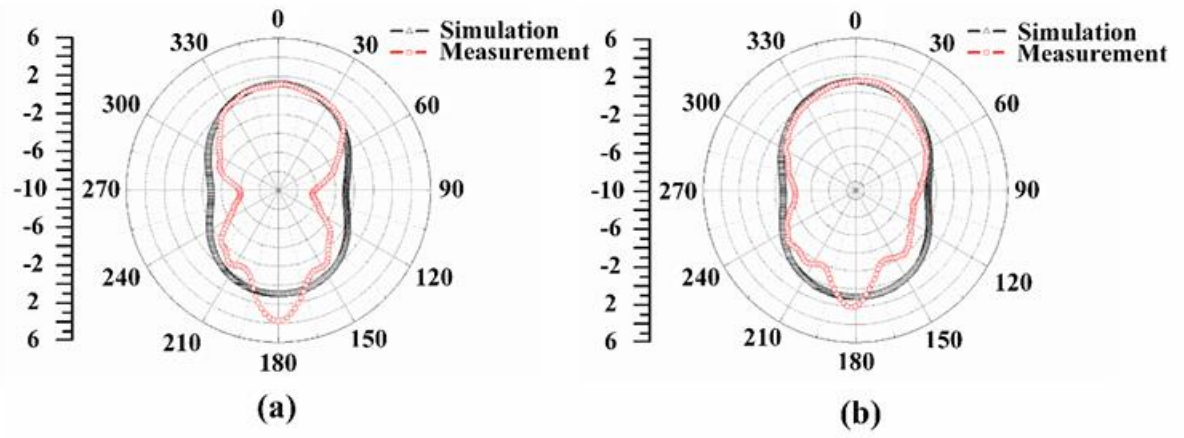

Fig. 3.Measured and Simulated Radiation Patterns at 1.550 GHz: (a) x-z Plane (b) y-z Plane.

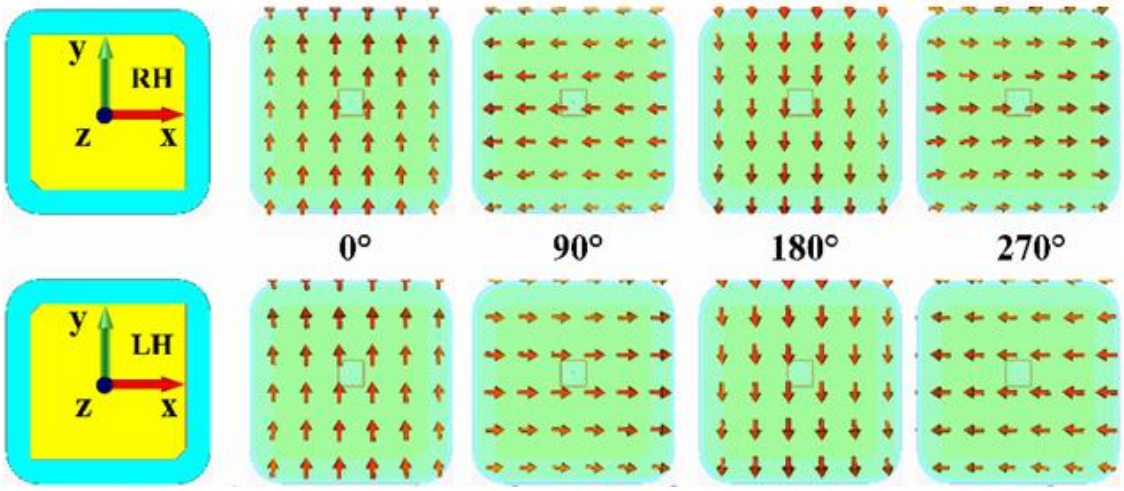

Fig. 4.Electric Field Vectors for Right-Hand Circular Polarization (RHCP) and Left-Hand Circular Polarization (LHCP) in One Period at 1.550 GHz.

In the design of the CP antenna, adopting the cut corner rectangle structure as radiation patch can help to realize the conversion between right hand (RH) CP and left hand (LH) CP. The conversion of the two states can be realized by simply changing the direction of cut corner. As shown in Figure 4, the electric field vectors for the antennas with different cut corner directions in one period obey the right-hand rule and left-hand rule, respectively. For the RHCP antenna, the Electric field vectors rotate counterclockwise a circle when the phase changes from 0° to 270°. In the case of LHCP antenna, there is a clockwise rotation, which means the transformation of CP state. The two CP states are used then to create the plus-and-negative mode OAM beams.

cognizancejournal.com
Mohammad Daud Ahmadzai *et al*, Cognizance Journal of Multidisciplinary Studies, Vol.5, Issue.1, January 2025, pg. 644-653
(An Open Accessible, Multidisciplinary, Fully Refereed and Peer Reviewed Journal)
ISSN: 0976-7797
Impact Factor: 5.183
Index Copernicus Value (ICV) = 77.57

Results: Antenna Array and the Generation of OAM Beams

Traditionally, to generate the OAM beam with mode of ±l, antennas are fed with signals of the same amplitude but different phases. The phase of the feeding signals is increased, in a turn, by $\pm 2\pi l$, where l is the mode of OAM beam. According to Nyquist theorem, a proper number of antennas needs to be greater than $2|l|+1$ [20]. Formation of OAM beams by CP antenna array are firstly reported in [31]. These OAM radio beams are considered as the mixture of two orthogonal line polarizations with 90° phase shifts. However, the complex structure is an obvious disadvantage of the CP antennas. And the application of the feed network makes the antenna array can operate only at a single frequency, thus limiting its flexibility. In our work, a GPS ceramic antenna array is used to generate OAM beams with the mode of ±1 at the resonant frequency of 1.550 GHz. The smallest number of components of the array is 4. However, the antenna number usually increases for standard waveform of the OAM beams. Therefore, six GPS ceramic antennas are suitable. It is worth noting that the antenna orientations are different with conventional ones. In the conventional method, the orientations of all antennas are the same [19,27]. Although the antennas in our system point to the center of the array. That is to say, the antennas are rotationally symmetric refer to the center. In this way, the antenna array can generate OAM beam through signals with the same amplitude and phase. Figure 5 dispaly the configuration of the antenna array and the imitation results. The RHCP antenna array described in Figure 5(a) includes of six RHCP GPS ceramic antennas evenly distributed on the circumference of a circle with $0.5\lambda 0$ radius. Imitation results of radiation pattern descibed in Figure 5(b) and phase delivery descibed in Figure 5(c) demonstrate that a standard OAM beam with mode of -1 is generated. Figures 5(d), (e) and (f) show the generation of OAM beam with mode of 1 when the antenna array involves of six LHCP GPS ceramic antennas. In addition, the polarization characteristic of GPS antenna is a benefit for OAM beam to reduce the divergence angle according to the radiation patterns. We can discover from Figure 5(b) and (e) that there is no sidelobe and small divergence angle in the radiation pattern of OAM beam with ±1, which mainly benefits from the small delivery radius of the antenna array and omnidirectional belongings of the CP antenna. These imitation results confirm the well performances of the GPS ceramic antenna array in generating OAM beams. It is worth mentioning that the axial ratio of the generated OAM is 19.8 dB. According to the successful experience of generating OAM beam with $l = \pm 1$, it is not hard to form beams with a large mode using the proposed method. We only need to change the phase difference $\Delta\varphi$ of adjacent antenna to $l \cdot \Delta\varphi$, where $\Delta\varphi = 2\pi/N$ (N is the antenna number of the array). For example, the antenna array used to the generate OAM beam with $l = 2$ is described in Figure 5(g). The array includes 1 RHCP antennas. Therefore, phase difference of adjacent antenna is set to 60°. The radioactivity pattern and phase distribution of the generated OAM beam are illustrated in Figure 5(h) and (i), respectively.

cognizancejournal.com
Mohammad Daud Ahmadzai *et al*, Cognizance Journal of Multidisciplinary Studies, Vol.5, Issue.1, January 2025, pg. 644-653
(An Open Accessible, Multidisciplinary, Fully Refereed and Peer Reviewed Journal)
ISSN: 0976-7797
Impact Factor: 5.183
Index Copernicus Value (ICV) = 77.57

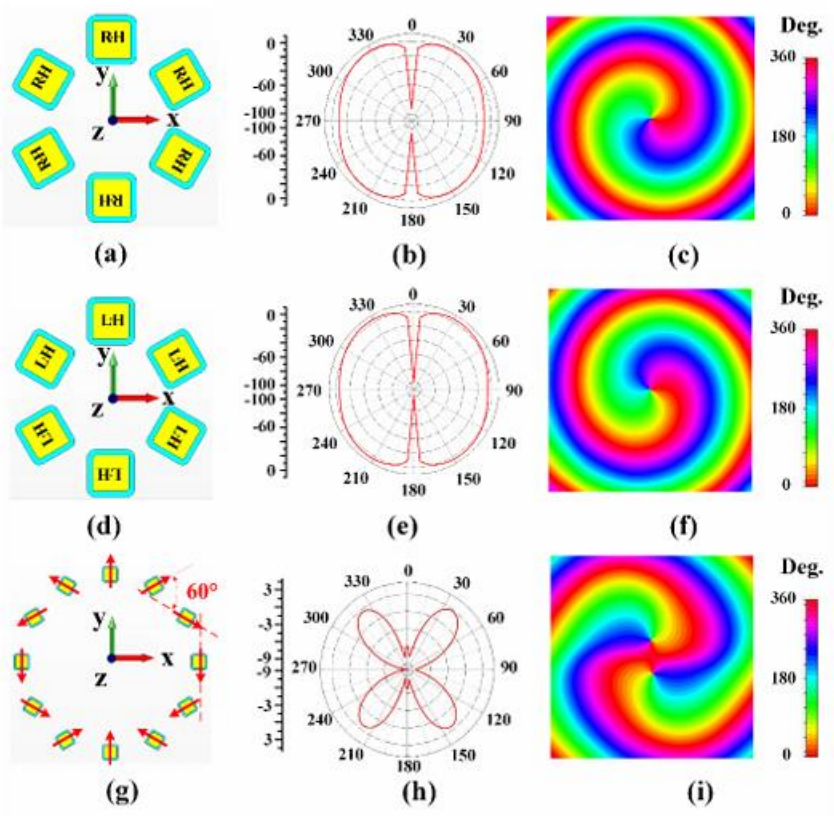

Fig. 5.Imitation of RHCP and LHCP Antenna Arrays at the Resonant Frequency of 1.550 GHz:

- (a) Formation of RHCP antenna array
- (b) Radioactivity pattern of RHCP antenna array in the y-z plane
- (c) Phase distribution of RHCP antenna array
- (d) Formation of LHCP antenna array
- (e) Radioactivity pattern of LHCP antenna array in the y-z plane
- (f) Phase distribution of LHCP antenna array
- (g) Formation of RHCP antenna array with 12 antennas
- (h) Radioactivity pattern of OAM beam with l = 2
- (i) Phase delivery of OAM beam with l = 2

cognizancejournal.com
Mohammad Daud Ahmadzai *et al*, Cognizance Journal of Multidisciplinary Studies, Vol.5, Issue.1, January 2025, pg. 644-653
(An Open Accessible, Multidisciplinary, Fully Refereed and Peer Reviewed Journal)
ISSN: 0976-7797
Impact Factor: 5.183
Index Copernicus Value (ICV) = 77.57

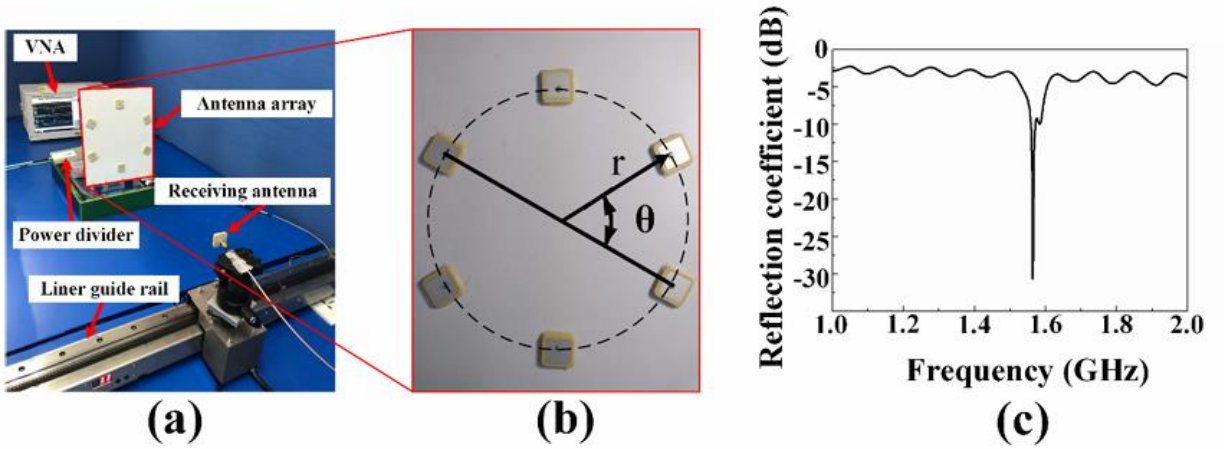

Fig. 6.Measurement System for OAM Beam Generation:

- (a) Overview of the measurement system for OAM beam creation
- (b) Details of the antenna array
- (c) Measured reflection coefficient of the proposed antenna array

Ulteriorly, an OAM beam measurement system is designed to detect the actual effect of OAM beam that created by an array connecting the GPS ceramic antenna. In this study, 6 GPS ceramic antennas with RHCP form the antenna array. It is similar in the case of LHCP. In the choice of the antenna number for the array, as odd will cause distortion of the OAM beam, the number of antennae need to be even. And the radius of antenna array r is 0.5λ0 to keep the array side lobes at low level and give enough space for each antenna. 6 antennas are regularly distributed on the circumference. So, the angle θ between antennas are 60°. The setup of the measurement system is described in Figure 6(a) and (b). A signal with the frequency of 1.550 GHz came from port 1 of vector network analyzer (VNA) is equally separated into 6 signals after passing a power divider. These signals are directly utilized to feed the antenna array with the help of coaxial lines. Then, the power and phase of the OAM beam with mode of -1 are detected by the receiving antenna with the help of liner guide rail. The center points of the guide rail and antenna array are both at z-axis, and the guide rail is parallel to the antenna array (x-y plane). Lastly, the sensed signal is transmitted back to port 2 of the VNA. To test the electromagnetic performance of the antenna array, the reflection constant is measured and the results are described in Figure 6(c). The agreement between Figure 6(c) and Figure 1 verifies the normal operation of the proposed antenna in the array and system.

cognizancejournal.com
Mohammad Daud Ahmadzai *et al*, Cognizance Journal of Multidisciplinary Studies, Vol.5, Issue.1, January 2025, pg. 644-653
(An Open Accessible, Multidisciplinary, Fully Refereed and Peer Reviewed Journal)
ISSN: 0976-7797
Impact Factor: 5.183
Index Copernicus Value (ICV) = 77.57

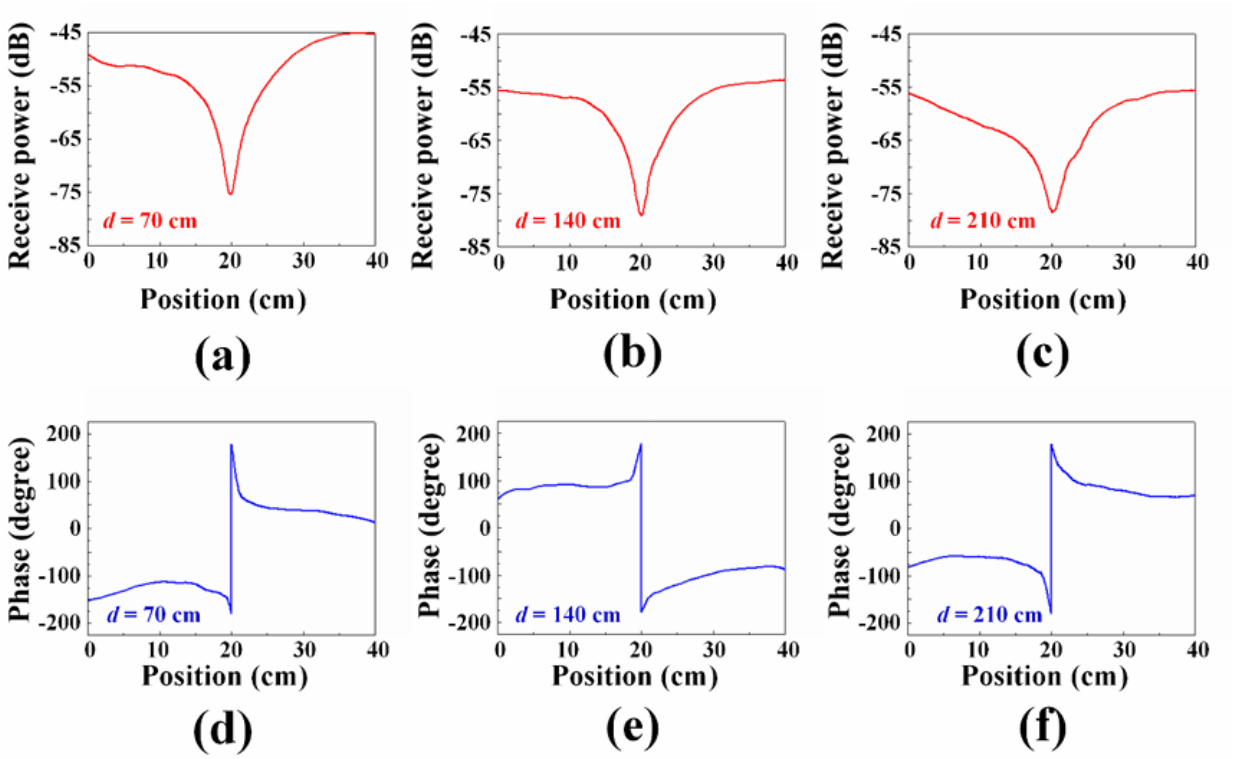

Fig. 7.Observed Receiving Power and Phase Distribution of the Generated OAM Beam at Various Distances from the Antenna Array:

- (a) Receiving power at 70 cm
- (b) Receiving power at 140 cm
- (c) Receiving power at 210 cm
- (d) Phase distribution at 70 cm
- (e) Phase distribution at 140 cm
- (f) Phase distribution at 210 cm

As mentioned above, a getting antenna and a liner guide rail are used to detect the one-dimensional spatial delivery of the OAM beam's electromagnetic characteristic at many distances away from the antenna array. The observed results are depicted in Figure 7, which includes a range from 0 to 40 cm. The sharp center decreases of the receiving powers and the 360° phase mutation in Figure 7 are obvious characteristics of OAM beam, which can be easily found in Figure 5. As shown in Figure 5, the sharp decrease and mutation emerge when the receiving antenna passes through the phase singularity. Because in this setup, the division of power and the long-distance transmission in cables cause enormous loss, the received powers shown in Figure 7 are low. However, by comparing Figure 7(a), (b) and (c), it can be found that the receive power only reduces a bit with the increase of the detection distance. Although the output power of VNA is only 0 dBm, the detectable distance can reach 210 cm.

Conclusion

A GPS ceramic antenna is designed and applied to generate OAM beam in radio domain. By changing the direction of the cut corner on the rectangle radiation patch, the CP state can be altered. A significantly simplified GPS ceramic antenna array with RHCP state is used to generate the OAM beam with negative mode. Similarly, GPS ceramic antenna array with LHCP state can generate the OAM beam with plus mode. By simulating the GPS ceramic antenna arrays, two kinds of OAM beams with standard spiral shape are successfully obtained. In particular, the radiation pattern of the OAM beam generated by the GPS ceramic antenna array shows quite small divergence angle and no side lobe, which confirms the excellent property of the antenna array in launching standard OAM beams. A series of experiments are designed and performed to test the electromagnetic characteristic of the OAM beams at different distances away from the antenna array. The OAM beams located at more than 2 meters away from the antenna array still can be detected when the output signal power is 0 dBm. After comparing with some recent periodicals, this approach is thought to be a great progress in the generation of high-quality OAM beam.

References

1. M. Padgett, and L. Allen, “Light with a twist in its tail,” Contemporary Physics, vol. 41, no. 5, pp. 275-285, 2000.
2. J. Leach, M. J. Padgett, S. M. Barnett et al., “Measuring the orbital angular momentum of a single photon,” Physical Review Letters, vol. 88, no. 1, pp. 257901, 2002.
3. J. Xu, M. Zhao, R. Zhang et al., “A wideband F-shaped microstrip antenna,” IEEE Antennas & Wireless Propagation Letters, vol. 16, pp. 829-832, 2016.
4. D. Mcgloin, N. B. Simpson, and M. J. Padgett, “Transfer of orbital angular momentum from a stressed fiber-optic waveguide to a light beam,” Applied Optics, vol. 37, no. 3, pp. 469, 1998.
5. M. Padgett, and R. Bowman, “Tweezers with a twist,” Nature Photonics, vol. 5, no. 6, pp. 343-348, 2011.
6. T. Yuan, H. Wang, Y. Qin et al., “Electromagnetic Vortex Imaging Using Uniform Concentric Circular Arrays,” IEEE Antennas & Wireless Propagation Letters, vol. 15, pp. 1024-1027, 2016.
7. L. Torner, J. P. Torres, and S. Carrasco, “Digital spiral imaging,” Optics Express, vol. 13, no. 3, pp. 873-81, 2005.
8. L. Paterson, M. P. Macdonald, J. Arlt et al., “Controlled rotation of optically trapped microscopic particles,” Science, vol. 292, no. 5518, pp. 912, 2001.
9. D. G. Grier, “A revolution in optical manipulation,” Nature, vol. 424, no. 6950, pp. 810-6, 2003.
10. H. Xu, K. Bi, Y. Hao et al., “Switchable Complementary Diamond-Ring-Shaped Metasurface for Radome Application,” IEEE Antennas and Wireless Propagation Letters, vol. 17, no. 12, pp. 2494-2497, 2018.
11. K. Bi, M. Bi, Y. Hao et al., “Ultrafine core-shell BaTiO3@SiO2 structures for nanocomposite capacitors with high energy densityof ferrite rods and metallic slits,” Nano Energy, vol. 51, pp. 513-523, 2018.
12. J. Wang, J. Y. Yang, I. M. Fazal et al., “Terabit free-space data transmission employing orbital angular momentum multiplexing,” Nature Photonics, vol. 6, no. 7, pp. 488-496, 2012.
13. F. Tamburini, E. Mari, A. Sponselli et al., “Encoding many channels in the same frequency through radio vorticity: first experimental test,” New Journal of Physics, vol. 14, no. 3, pp. 811-815, 2011.
14. X.T. Wang, Y. Cui, T. Li et al., “Recent advances in the functional 2D photonic and optoelectronic devices,” Advanced Optical Materials, DOI: 10.1002/adom.201801274.
15. S. Yu, L. Li, G. Shi et al., “Design, fabrication, and measurement of reflective metasurface for orbital angular momentum vortex wave in radio frequency domain,” Applied Physics Letters, vol. 108, pp. 121903, 2016.
16. S. Lin, X.P. Bai, H.Y. Wang et al., “Roll-to-Roll Production of Transparent Silver Nanofiber Network Electrode for Flexible Electrochromic Smart Windows,” Advanced Materials, vol. 29, pp. 1703238, 2017.
17. N. Bozinovic, Y. Yue, Y. Ren et al., “Terabit-scale orbital angular momentum mode division multiplexing in fibers,” Science, vol. 340, no. 6140, pp. 1545, 2013.

18. K. Bi, W. T. Zhu, M. Lei et al., "Magnetically tunable wideband microwave filter using ferrite-based metamaterials," Applied Physics Letters, vol. 106, pp. 173507, 2015.
19. Q. Wang, X. Li, L.Y. Wu et al., "Electronic and Interface Properties in Graphene Oxide/Hydrogen-Passivated Ge Heterostructure," Physica Status Solidi RRL, DOI: 10.1002/pssr.201800461.
20. B. Thidé, H. Then, J. Sjöholm et al., "Utilization of photon orbital angular momentum in the low-frequency radio domain," Physical Review Letters, vol. 99, no. 8, pp. 087701, 2007.
21. A. Tennant, and B. Allen, "Generation of OAM radio waves using circular time-switched array antenna," Electronics Letters, vol. 48, no. 21, pp. 1365-1366, 2012.
22. P. Schemmel, G. Pisano, and B. Maffei, "Modular spiral phase plate design for orbital angular momentum generation at millimetre wavelengths," Optics Express, vol. 22, no. 12, pp. 14712, 2014.
23. X. Hui, S. Zheng, Y. Hu et al., "Ultralow Reflectivity Spiral Phase Plate for Generation of Millimeter-wave OAM Beam," IEEE Antennas & Wireless Propagation Letters, vol. 14, pp. 966-969, 2015.
24. F. Tamburini, E. Mari, T. Bo et al., "Experimental verification of photon angular momentum and vorticity with radio techniques," Applied Physics Letters, vol. 99, no. 20, pp. 321, 2011.
25. L. Cheng, W. Hong, and Z. C. Hao, "Generation of electromagnetic waves with arbitrary orbital angular momentum modes," Scientific Reports, vol. 4, pp. 4814, 2014.
26. Q. Bai, A. Tennant, and B. Allen, "Experimental circular phased array for generating OAM radio beams," Electronics Letters, vol. 50, no. 20, pp. 1414-1415, 2014.
27. X. Gao, S. Huang, Y. Wei et al., "An orbital angular momentum radio communication system optimized by intensity controlled masks effectively: Theoretical design and experimental verification," Applied Physics Letters, vol. 105, pp. 241109, 2014.
28. L.Y. Wu, P.F. Lu, R.G. Quhe et al., "Stanene Nanomeshes as Anode Materials for Na-ion Batteries," Journal of Materials Chemistry A, vol. 6, pp. 7933, 2018.
29. O. P. Falade, M. U. Rehman, Y. Gao et al., "Single Feed Stacked Patch Circular Polarized Antenna for Triple Band GPS Receivers," IEEE Transactions on Antennas & Propagation, vol. 60, no. 10, pp. 4479-4484, 2012.
30. Y. Huang, L. Yang, J. Li et al., "Polarization conversion of metasurface for the application of wide band low-profile circular polarization slot antenna," Applied Physics Letters, vol. 109, no. 5, pp. 917, 2016.
31. F. Spinello, E. Mari, M. Oldoni et al., "Experimental near field OAM-based communication with circular patch array," arXiv:1507.06889 [physics.optics].
32. X. D. Bai, X. L. Liang, Y. T. Sun et al., "Experimental Array for Generating Dual Circularly-Polarized Dual-Mode OAM Radio Beams," Scientific Reports, vol. 7, pp. 40099, 2017.
33. G. Xie, Z. Zhao, Y. Yan et al., "Demonstration of Tunable Steering and Multiplexing of Two 28 GHz Data Carrying Orbital Angular Momentum Beams Using Antenna Array," Scientific Reports, vol. 6, pp. 37078, 2016.
34. C. Xu, S. Zheng, W. Zhang et al., "Free-Space Radio Communication Employing OAM Multiplexing Based on Rotman Lens," IEEE Microwave & Wireless Components Letters, vol. 26, no. 9, pp. 738-740, 2016.
35. G. Xinlu, H. Shanguo, S. Yunlong et al., "Generating the orbital angular momentum of radio frequency signals using optical-true-time-delay unit based on optical spectrum processor," Optics Letters, vol. 39, no. 9, pp. 2652-5, 2014.
36. K. Liu, H. Liu, Y. Qin et al., "Generation of OAM Beams Using Phased Array in the Microwave Band," IEEE Transactions on Antennas & Propagation, vol. 64, no. 9, pp. 3850-3857, 2016.
37. Y. Gong, R. Wang, Y. Deng et al., "Generation and Transmission of OAM-Carrying Vortex Beams Using Circular Antenna Array," IEEE Transactions on Antennas & Propagation, vol. 65, no. 6, pp. 2940-2949, 2017.
38. H. Yao, H. Kumar, T. Ei et al., "Patch Antenna Array for the Generation of Millimeter-wave Hermite-Gaussian Beams," IEEE Antennas & Wireless Propagation Letters, vol. 15, pp. 1947-1950, 2016.
39. B. Y. Liu, Y. H. Cui, and R. Li, "A Broadband Dual-Polarized Dual-OAM-Mode Antenna Array for OAM Communication," IEEE Antennas & Wireless Propagation Letters, vol. 16, pp. 744-747, 2017.
40. Z. G. Guo, and G. M. Yang, "Radial Uniform Circular Antenna Array for Dual-Mode OAM Communication," IEEE Antennas & Wireless Propagation Letters, vol. 16, pp. 404-407, 2017.

